

## High-Throughput Laser Diode Thermal Desorption-Tandem Mass Spectrometry Method for Rapid Determination of Lamotrigine in Human Plasma

Glauco César F. F. Soares,<sup>\*,a,b</sup> Danilo F. M. C. Veloso,<sup>1b a,c</sup> Iram M. Mundim,<sup>a</sup> Leonardo S. Teixeira,<sup>a</sup> Maria Carolina Almeida<sup>1b d</sup> and Luiz Carlos da Cunha<sup>b</sup>

<sup>a</sup>Instituto de Ciências Farmacêuticas, Alameda Coronel Eugênio Jardim, 53, 74175-100 Goiânia-GO, Brazil

<sup>b</sup>Núcleo de Estudos e Pesquisas Tóxico-Farmacológicas (NEPET), Universidade Federal de Goiás, 74605-170 Goiânia-GO, Brazil

<sup>c</sup>Secretaria de Estado da Educação do Estado de Goiás (SEDUC), Av. Quinta Avenida, quadra 71, No. 212, Setor Leste Vila Nova, 74643-030 Goiânia-GO, Brazil

<sup>d</sup>Instituto Federal de Educação, Ciência e Tecnologia (IFG), Campus Inhumas, Avenida Universitária, Vale das Goiabeiras, 75402-556 Inhumas-GO, Brazil

We present the development and validation of a laser diode thermal desorption coupled with mass spectrometry (LDTD-MS/MS) as a high-throughput method for bioanalysis. This technique was applied clinically to determine the pharmacokinetics (PK) of the anticonvulsant drug lamotrigine (LAM) after administering two different oral formulations. Our method offers significant advantages over liquid chromatography in terms of sustainability. Sample preparation required just 50  $\mu\text{L}$  of human plasma. Liquid-liquid extraction (LLE) overcomes protein precipitation for sample cleanup while avoiding any compromise in the desorption and ionization of LAM, thereby eliminating the need for microwell surface coating. This validated, internationally compliant method provided ultra-rapid LAM plasma level determination, with a 10 s runtime *per* sample. The linearity range of 20-2000  $\text{ng mL}^{-1}$  effectively enabled the full capture of the PK profile of 36 volunteers. Such findings highlight the versatility of this approach, demonstrating its potential to align with evolving regulatory standards and potentially paving the way for its broader adoption in routine bioanalysis.

**Keywords:** pharmacokinetics, ultrafast analysis, bioanalysis, drug monitoring, clinical application

### Introduction

Analytical methods based on laser diode thermal desorption (LDTD) have demonstrated remarkable versatility and effectiveness, encompassing a wide range of applications. When integrated with mass spectrometry (MS/MS), LDTD significantly enhances the efficiency of analytical method development, making it an invaluable tool in bioanalytical science.<sup>1-5</sup>

In the current landscape, there is an increasing demand for analytical methods that deliver precision and sensitivity and align with sustainability principles.<sup>6</sup> These capabilities are crucial for tackling time-sensitive challenges like

expiring drug patents and giving a competitive edge to pharmaceutical companies by quickly launching generic products.<sup>7-11</sup>

While liquid chromatography mass spectrometry (LC-MS/MS) remains the gold standard in bioanalysis owing to its high selectivity, sensitivity, and precision, its analysis time (1-20 min) is limited by automated steps such as sample injection, washing cycles, and chromatographic separation.<sup>12-17</sup>

Unlike classical LC methods, LDTD-MS/MS obviates the reliance on organic solvents, streamlines sample preparation, reduces cross-contamination, and enhances reproducibility.<sup>1,17</sup>

In LDTD-MS/MS, samples are spotted onto a 96-microwell plate, evaporated, and thermally desorbed by an infrared laser. The vaporized analytes are then carried by

\*e-mail: glauco.faria@icf.com.br

Editor handled this article: Andréa R. Chaves (Associate)



gas to an atmospheric pressure chemical ionization source and analyzed by the mass spectrometer.<sup>1</sup>

Analyte desorption and ionization from the LDTD plate can be significantly improved by using a microwell surface coating.<sup>18</sup> Typically composed of stabilizers like bovine serum albumin and surface modifiers such as potassium phosphate,<sup>19-21</sup> the coating enhances energy transfer, promotes uniform laser pulse absorption, and reduces thermal degradation and fragmentation. As a result, it improves analyte ionization, stability, and overall performance.<sup>22-25</sup>

LDTD-MS/MS offers a streamlined approach to sample analysis by bypassing the time-consuming LC separation step.<sup>26</sup> This speeds up sample processing and analysis while reducing costs associated with chromatographic consumables turnover, particularly for biological sample analysis. Despite advancements, the principle of the LDTD-MS/MS method relies on thermal desorption and restricts its use with thermally unstable analytes.<sup>27-29</sup>

Furthermore, the lack of chromatographic separation can hinder calibration and quantification due to matrix interferences, reducing specificity and impairing the differentiation of structurally similar compounds or isomers. These limitations highlight the importance of careful analyte screening and evaluating the suitability of the method for bioanalytical studies.<sup>27,30</sup>

In this study, lamotrigine (LAM), an anticonvulsant drug prescribed for epilepsy and bipolar disorder, is evaluated using the approach mentioned, given its unique physicochemical properties. These properties make it an excellent candidate for precise quantification in complex biological matrices via LDTD-MS/MS.<sup>31,32</sup> LAM is rapidly and completely absorbed after oral administration, with nearly 100% bioavailability. However, plasma levels can fluctuate significantly as a result of factors like drug interactions and pregnancy, highlighting the need for therapeutic monitoring.<sup>33,34</sup>

Therefore, this study aims to develop and validate a rapid bioanalytical method for LAM quantification in human plasma employing a high-throughput LDTD-MS/MS instrument.

## Experimental

### Materials

LC-MS/MS grade, methanol, acetonitrile, methyl *tert*-butyl ether, and formic acid (99.5%) were products of J. T. Baker (Phillipsburg, NJ, USA). Water was obtained using a Milli-Q system (Millipore, Billerica, MA, USA) equipped with a 0.22 mm pore end-filter. Bovine serum albumin, potassium phosphate, and United States

Pharmacopoeia (USP) reference standards LAM and carbamazepine were acquired from Sigma-Aldrich Co (St. Louis, MO, USA). Reference drug at the dose of 100 mg is a product of GSK (Rio de Janeiro, RJ, Brazil) that was purchased in local market.

### Methods

Preparation of standard solutions: stock solutions of LAM and carbamazepine, used as the internal standard (IS), were prepared in acetonitrile (ACN) at a concentration of 10.000 ng mL<sup>-1</sup>. Standard working solutions for calibration were prepared by appropriate dilution with ACN:H<sub>2</sub>O (1:1, v/v) from the stock solution, resulting in LAM concentrations of 20; 60; 200; 500; 1000; 1200; and 2000 ng mL<sup>-1</sup>. Quality control (QC) samples were prepared at three concentrations: low (LQC), medium (MQC), and high (HQC) at a concentration of 60; 1000, and 1600 ng mL<sup>-1</sup>, respectively. IS working solution at 2000 ng mL<sup>-1</sup> was prepared in the same way.

### Mass spectrometry LDTD optimization

LAM and IS were detected and quantified using an API6500 triple quadrupole mass spectrometer MDS-SCIEX (Concord, Ontario, Canada). The setup for both drugs comprised a dwell time of 70 ms *per* transition; the curtain gas was set to 10 and the collision-activated dissociation (CAD) gas level adjusted to medium. Additional MS conditions included collision exit potential of 24 V for LAM and 22 V for IS, and a collision energy of 35 for LAM and 25 for IS, respectively. Multiple reaction monitoring (MRM) was employed to enhance the sensitivity and specificity of drug detection. For each drug, the two most abundant transitions were monitored in MRM mode, with one transition from each drug selected for further validation. LDTD Phytronix Technologies (Quebec, Canada) source operation involved configuring the carrier gas flow at 6.0 L min<sup>-1</sup> and establishing the final laser pattern at 70%, initiated by a gradual increase from 68%. Data acquisition and processing were obtained using Analyst<sup>®</sup> software<sup>35</sup> version 1.7.2 (AB SCIEX, Framingham, MA).

### Sample preparation and extraction procedure

Protein precipitation was used as a mixture of 50 µL of plasma, 10 µL of standard solution (at 60 ng mL<sup>-1</sup>), and 10 µL of IS solution (at 2000 ng mL<sup>-1</sup>) in 400 µL of methanol as the precipitating solvent. Subsequently, the resulting mixture was vigorously vortexed for 5 min. The obtained solution was then centrifuged at 12000 rpm for 10 min.

Liquid-liquid extraction (LLE) was also used by adding 50  $\mu\text{L}$  of plasma, 10  $\mu\text{L}$  of standard solution, and 10  $\mu\text{L}$  of IS at the same concentration of protein precipitation assay, combined in a 2.0 mL Eppendorf tube. Subsequently, 1250  $\mu\text{L}$  of methyl *tert*-butyl ether (MTBE) were added, and the mixture was stirred for 2 min. Following, the solution was centrifuged at 12000 rpm for 10 min to assist with phase separation. In a Phytronix LazWell® 96-microwell plate (Phytronix Technologies, Quebec, Canada), 180  $\mu\text{L}$  of the extracted sample were spotted and dried at 40 °C using a dry block. Then, the dried samples were reconstituted with 100  $\mu\text{L}$  of a methanol:water mixture (1:1, v/v) and shaken for 8 s at 1200 rpm using a thermo-shaker. In both extraction methods, any calibration standard and quality control sample required spiking 10  $\mu\text{L}$  of standard solution into plasma. This step was not applied to clinical samples.

After sample cleanup, desorption efficiency was optimized under laser irradiation by spotting 2.5  $\mu\text{L}$  of the obtained solution onto the Phytronix LazWell® 96-microwell plate and dried for 5 min under a gentle stream of nitrogen before the LDTD-MS/MS analysis.

To enhance the ionization and stability of the extracted sample, 2.5  $\mu\text{L}$  of a substrate mixture (100  $\mu\text{g mL}^{-1}$  bovine serum albumin and 1 mM potassium phosphate) were incorporated into the obtained solution and placed in the microwell. This process is referred to as microwell surface coating.

#### Validation process

The validity of the bioanalytical method was confirmed by approaches in compliance with the FDA Bioanalytical Method Validation Guidance for Industry<sup>36</sup> guidelines, as well as the recommendations put forth by Visconti *et al.*,<sup>37</sup> the Brazilian regulatory agency, Agência Nacional de Vigilância Sanitária (ANVISA),<sup>38</sup> and aligned with the principles established by the International Council for Harmonisation (ICH).<sup>39</sup> The assessment encompassed various parameters including selectivity, linearity, limits of detection and quantification, bias, precision, matrix effect, carry-over, and sample stability in different stress and storage conditions.

#### Matrix effect

The matrix effect was evaluated at LQC and HQC levels. A total of 16 human plasma samples for each concentration were used in this assay, consisting of 8 batches: 4 normal, 2 hemolyzed, and 2 lipemic. The other set of 8 human plasma samples with the same composition was prepared, each one spiked with common over-the-counter drugs at the following concentrations: paracetamol

(20000.00 ng mL<sup>-1</sup>), caffeine (1000.00 ng mL<sup>-1</sup>), scopolamine butyl bromide (2.00 ng mL<sup>-1</sup>), 4-methylamino antipyrine (8000.00 ng mL<sup>-1</sup>), cotinine (1500.00 ng mL<sup>-1</sup>), and ondansetron (1500.00 ng mL<sup>-1</sup>). The human plasma samples were processed following the procedure outlined in the “Sample preparation and extraction” sub-section. After extraction, the matrix was spiked with LAM at concentrations equivalent to the LQC and HQC levels. Mean peak areas of LAM in the spiked blank matrix and in ACN:H<sub>2</sub>O (1:1, v/v) solution were obtained. The procedure for validating this parameter necessitates the acquisition of the normalized matrix factor (NMF) from both QCs. NMF results are obtained following the equation 1:

$$\text{NMF} = \frac{\text{analyte peak area in matrix/IS peak area in matrix}}{\text{analyte peak area in solution/IS peak area in solution}} \quad (1)$$

Subsequently, the coefficient of variation (CV) in percentage, for the NMFs of LQC and HQC samples should be computed, ensuring it remains below 15% (fifteen percent), as stipulated by ANVISA.<sup>38</sup>

#### Specificity

The potential interference of endogenous plasma components and concomitant medications with LAM and IS ionization was evaluated. The assessment involved 12 human blank plasma samples, divided into two sets. The first set included six batches (four normal, one hemolyzed, and one lipemic). The second set consisted of six similarly composed batches spiked with concomitant drugs used in the matrix effect assay. All samples were processed and analyzed according to the proposed extraction protocol and the established equipment conditions for LAM and IS. The specificity of the method was considered acceptable if, in the different blank plasma samples, no desorption peak exhibited an area exceeding 20% of the LLOQ area for LAM or 5% of the IS area.

#### Carry-over

In this assay, a blank plasma sample was analyzed three times. The first analysis was conducted before any setup to establish a baseline. Subsequently, two additional analyses of the blank plasma sample were performed immediately after the analysis of the ULOQ, which contained the IS at a concentration of 2000 ng mL<sup>-1</sup>. For reference, a lower limit of quantitation (LLOQ) sample was also analyzed, and its peak area was used as a benchmark. Carry-over was considered significant if the desorption peak area of the blank plasma sample exceeded 20% of the LLOQ peak area or 5% of the IS peak area.

## Sensitivity and linearity

The linearity range was determined by considering the maximum plasma concentration of the drug over time ( $C_{\max}$ ) obtained from prior pharmacokinetics (PK) and bioequivalence studies.<sup>40-42</sup> It was ensured that the range analyzed was not excessively narrow and did not exceed values achievable in volunteers, covering the full PK profile of a single dose of LAM orally administered. Linearity was examined by analyzing duplicate calibration standards across seven concentration levels over three consecutive days. The curves were generated by plotting the peak area ratio of LAM to the IS against each respective concentration.

Determination of the calibration curve was undertaken through least squares analysis. The calibration curve was deemed acceptable only if the residuals fell within a 20% margin at the LLOQ and within a 15% margin at all other calibration levels, with a stipulation that at least two-thirds of the calibration standards adhered to this criterion, accounting for both the highest and lowest concentrations. For the sensitivity of the assay, the LLOQ was established at the concentration where precision and accuracy were upheld within a 20% threshold, as determined through the analysis of seven replicates. Precision was characterized by the coefficient of variation, and accuracy, denoted by the relative deviation expressed as a percentage error from the target concentrations, was assessed across LLOQ (20 ng mL<sup>-1</sup>) and all three-quality control (QC) levels of 60, 1000, and 1600 ng mL<sup>-1</sup>. Intra-run accuracy and precision were assessed by analyzing three replicates of samples at the LLOQ and each QC level on the same day. Inter-run accuracy and precision were evaluated using three replicates ( $n = 3$ ) *per* concentration across three days.

Linearity was assessed within the standard concentration range of 20-2000 ng mL<sup>-1</sup> in human plasma. The correlation between peak area ratio and LAM nominal concentration was determined using  $1/x^2$  weighted linear regression. To establish the calibration curve, the accuracies of at least 75% of the calibration standards, including the LLOQ and ULOQ, had to fall within the  $\pm 15.0\%$  range ( $\pm 20.0\%$  at LLOQ), and the correlation coefficient ( $r^2$ ) needed to be greater than 0.99. The lowest concentration on the calibration curve that could be reliably determined was then determined.

## Stability assessments

Stability assessment of LAM and IS in human plasma involved exposure to different storage and stress conditions,<sup>43</sup> including four complete freeze-thaw cycles ( $-70 \pm 15$  °C to room temperature, approximately 20 °C for 45 min, back to  $-70 \pm 15$  °C, and stored for 24 h),

short-term bench stability (ca. 4 h), and autosampler stability (1.93 h), under controlled laboratory conditions (approximately 20 °C) and long-term stability 2.5 months at  $-70 \pm 15$  °C. Stability studies were conducted at low and high QC levels (60 and 1600 ng mL<sup>-1</sup>, respectively) in six replicates. Stability was deemed acceptable when the concentrations of stored stability samples remained within 85 to 115% of their nominal values. This was assessed by comparing them to freshly prepared calibration curves and QC samples, with results expressed as relative error (RE) in percentage.

## Method application in comparative PK of LAM tablets

The clinical trial was designed as a monocentric, open-label, crossover, randomized study with two arms treatment (reference and test), two sequences (reference-test and test-reference), and two periods. It was conducted under truncated fasting conditions, focusing on a single subgroup of 36 healthy volunteers of both sexes. Each participant received a single dose of either the reference drug or the test formulation, in an equivalent dose of 100 mg of LAM tablets. Blood samples were collected using ethylenediaminetetraacetic acid (EDTA) as an anticoagulant at pre-dose and specific post-dose time points: 0.25, 0.5, 0.75, 1, 1.25, 1.5, 2, 2.5, 3, 3.5, 4, 5, 6, 8, 12, 24, 48, 72 and 96 h. Immediately after collection, samples were centrifuged at 3,000 rpm for 5 min. The plasma supernatant was carefully separated and stored at  $-70 (\pm 15$  °C) within 2 h of centrifugation. Subsequently, LAM was extracted from the plasma samples using the previously described extraction methods, followed by analysis using LDTD-MS/MS. The protocol number of the trial 5.610.806 was approved by the research ethics Committee of Instituto de Ciências Farmacêuticas. Primary PK parameters were determined using non-compartmental analysis in Phoenix WinNonlin<sup>®44</sup> v.6.4.0.768 (Pharsight, Mountain View, CA).

## Results and Discussion

### Sample preparation and LDTD-MS/MS detection

The monitoring of LAM was carried out using the most intense precursor-to-product ion transition ( $m/z$  256.2  $\rightarrow$   $m/z$  211.0). Figure 1a illustrates the precursor ion, corresponding to the protonated molecules  $[M + H]^+$ . Following collision-induced dissociation, the most stable and abundant fragment is observed in Figure 1b, which corresponds to the cleavage of the triazine ring from the protonated molecule in positive ion mode during MRM.<sup>45</sup>

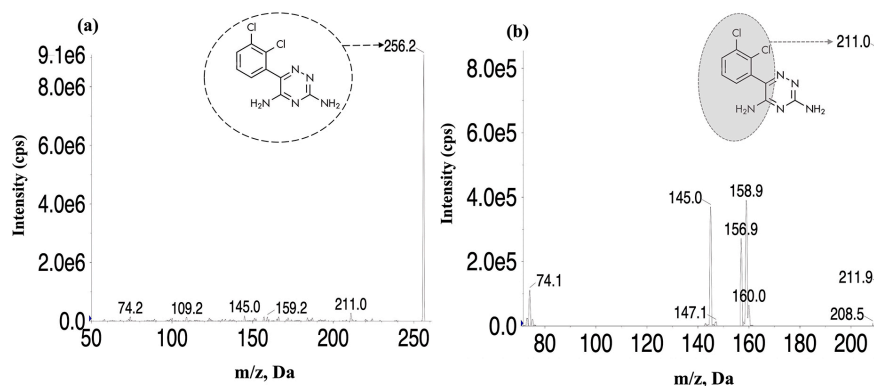


**Figure 1.** Representative mass spectrum of LAM obtained in positive ionization mode, showing the precursor ion (a) at  $m/z$  256.2 Da and the product ion (b) at  $m/z$  211.0 Da. MS data were acquired under the following parameters: a dwell time of 70 ms, a curtain gas flow rate of 10, and the CAD gas was adjusted to medium. The collision exit potential was 24 V, and the collision energy was set to 35 V. To enhance sensitivity and specificity, multiple reaction monitoring (MRM) mode was employed. The relative abundance of the selected ions is measured in counts *per s* (cps).

Refining the sample preparation protocol is pivotal for optimizing LDTD-MS/MS analysis,<sup>46,47</sup> as demonstrated in this study. Remarkable differences observed in plasma samples subjected to different extraction methods are shown in Figures 2 and 3. Notably, protein precipitation extraction yielded distinct peaks for both LAM (Figure 2a) and IS (Figure 2b). However, in the blank plasma samples (Figures 2c and 2d), a sharp peak is evident in Figure 2c, likely due to interference from the matrix.

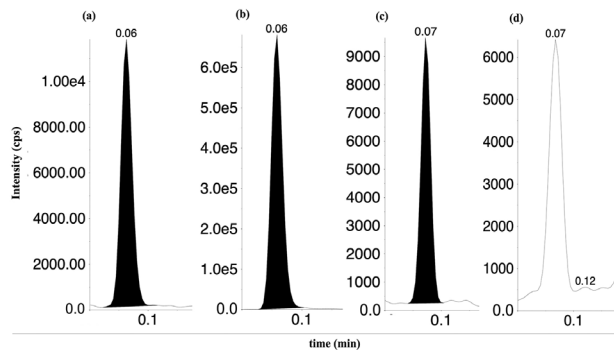


**Figure 2.** Desorption profiles for LAM and IS by protein precipitation (using microwell surface coating and the laser power set at 68%): (a) desorption peak for LAM-containing sample, (b) desorption peak for IS-containing sample, (c) LAM desorption peak observed in the blank plasma sample, and (d) no desorption peak detected in the blank plasma sample for IS. Desorption peaks were detected between 0.06–0.07 min at 60 and 2000 ng mL<sup>-1</sup> concentrations for LAM and IS, respectively. The y-axis represents the desorption peak intensity, measured in counts *per s* (cps).

Conversely, while LLE excelled in impurity removal, the incorporation of microwell surface coating, comprising a solvent-matrix-cationized salt blend aimed at enhancing ionization yielded unexpected outcomes.<sup>48</sup>

In contrast to the ionization enhancement observed with the microwell surface coating in the precipitation extraction assay, its use in LLE appeared counterproductive, suppressing ionization and causing a significant reduction

in signal intensity (Figures 3a and 3b). Nevertheless, the use of LLE for sample cleanup significantly reduced interference in the LAM analysis channel, as no desorption peaks were observed in Figures 3c and 3d, demonstrating its superior efficacy in sample purification.<sup>49,50</sup>

To address the potential ionization suppression caused by the microwell surface coating in LLE samples, the laser power was strategically increased. This adjustment effectively enhanced the peak intensity (Figures 3e and 3f), resulting in no interferences at LAM and IS desorption times (Figures 3g and 3h). As a result, the analysis became more accurate and selective, eliminating the need for reliance on the microwell surface coating in the samples.

The increased laser intensity enhanced the energy transfer to the sample and the amount of material thermally desorbed into the gas phase, significantly minimizing the impact of interfering contaminants released during desorption. In addition, the favorable ionization properties of LAM, combined with its well-documented stability under heat, humidity, and light conditions, make this drug a viable choice for analysis using LDTD-MS/MS.<sup>18,32,51</sup>

Moreover, LLE proved to be highly effective, yielding optimal results for LAM analysis. Using 50  $\mu$ L of human plasma minimizes biological material use while ensuring sufficient matrix representation. Although a relatively large volume of 1250  $\mu$ L of organic solvent was used in the extraction process, this solvent plays a crucial role in effectively cleaning up the plasma sample while maximizing the partitioning of LAM. Since chromatographic separation is not employed, this approach ensures reliable quantification by balancing drug solubility, matrix cleanup, and method compatibility.<sup>52</sup> Given these findings, the method was validated using LLE and eliminating the additional microwell surface coating step. This optimization strategy represents a crucial advancement in LDTD-MS/MS analysis, ensuring accurate and reliable detection of LAM.

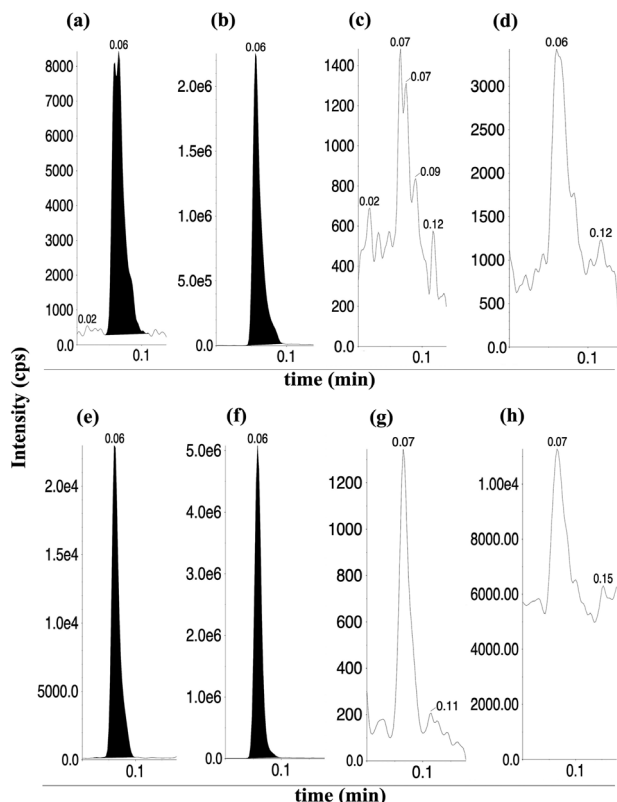


**Figure 3.** Desorption profiles for LAM and IS in LLE (using microwell surface coating and the laser power set at 68%): (a) desorption peak for LAM-containing sample, (b) desorption peak for IS-containing sample, (c) no desorption peak observed in the blank plasma sample for LAM, and (d) no desorption peak detected in the blank plasma sample for IS. For LLE (uncoated samples and the laser power set at 70%): (e) prominent desorption peak for LAM-containing sample, (f) prominent desorption peak for IS-containing sample, (g) no desorption peak observed in the blank plasma sample for LAM, and (h) no desorption peak detected in the blank plasma sample for IS. Desorption peaks were detected between 0.06–0.07 min at 60 and 2000 ng mL<sup>-1</sup> concentrations for LAM and IS, respectively. The y-axis represents the desorption peak intensity, measured in counts *per s* (cps).

### Method validation process

Sensitivity and linearity: LAM met the ANVISA<sup>38</sup> acceptance criteria with a seven-point calibration curve.

**Table 1.** Intra-run and inter-run precision and accuracy results of LAM in human plasma using LDTD-MS/MS analysis

LAM nominal concentration / (ng mL <sup>-1</sup> )	Intra-run			Inter-run		
	Measured concentration ± SD / (ng mL <sup>-1</sup> )	Precision / %	Accuracy / %	Measured concentration ± SD / (ng mL <sup>-1</sup> )	Precision / %	Accuracy / %
20 (LLOQ)	19.3 ± 2.1	10.88	-3.50	18.3 ± 2.3	12.57	-8.50
60 (LQC)	59.6 ± 6.9	11.58	-0.67	61.1 ± 5.4	8.84	1.83
1000 (MQC)	992.2 ± 118.9	11.98	-0.78	1000.0 ± 90.0	9.00	0.00
1600 (HQC)	1547.1 ± 116.4	7.52	-3.31	1595.8 ± 130.8	8.20	-0.26

LAM: lamotrigine; SD: standard deviation; LLOQ: lower limit of quantification; LQC: low concentration; MQC: medium concentration; HQC: high concentration.

Calibration curves exhibited excellent linearity across the investigated concentration range (20–2000 ng mL<sup>-1</sup>), boasting correlation coefficients ( $r^2$ ) surpassing 0.99 in all instances.

Furthermore, all back-calculated standard concentrations fell within a 15% deviation from the nominal value, meeting the stringent criterion set at a maximum allowable deviation of 20%, even at the LLOQ. Notably, the residuals displayed no discernible trend concerning to concentration. The precision and accuracy data for intra- and inter-run analyses are succinctly presented in Table 1. Based on these results, the assay demonstrates both accuracy and precision for LAM within the explored concentration range.

Intra-run results were obtained by analyzing three replicates of samples at the LLOQ and each QC level within a single day. Inter-run results involved three replicates *per* concentration analyzed across three consecutive days. The LLOQ (lower limit of quantification) was set at 20 ng mL<sup>-1</sup>, while QC levels included low (LQC, 60 ng mL<sup>-1</sup>), medium (MQC, 1000 ng mL<sup>-1</sup>), and high (HQC, 1600 ng mL<sup>-1</sup>). Measured concentrations are reported as means ± standard deviation ( $n = 3$  *per* concentration).

### Matrix effect

The normalized matrix factor (NMF) results obtained for the LQC level were  $0.78 \pm 0.070$ , while for the HQC level, they were  $0.02 \pm 0.00$ . In both cases, the CV was within the acceptable limit of 15%, as established by ANVISA<sup>38</sup> guidelines. Specifically, the CV values were 8.32 and 7.12% for the LQC and HQC NMF, respectively. These results demonstrate compliance with the regulatory threshold and confirm the absence of significant matrix interference in determining the LAM and IS desorption peak areas. In this fashion, no evidence of matrix effects at any analyzed concentrations of the monitored drug and IS arises from the interplay between the impact of the matrix on the ion source or their chemical characteristics.

## Specificity

Outcomes of the specificity test underscored the absence of contamination exceeding 20% of the LLOQ peak area for LAM within the desorption peaks detection window (0.06 min) across all analyzed samples. Blank plasma samples, regardless of their normal, lipemic, or hemolyzed state, displayed contamination levels ranging from 1.54 to 5.68% of the LLOQ area. Additionally, the same aforementioned plasma batches contaminated with the drugs outlined in the methodology exhibited contamination limits capped at 15.35% of the LLOQ area. Concerning the IS, the desorption peak areas detected at 0.05 min ranged from 0.13 to 0.34%, remaining within the predefined 5.0% limit for the IS.

## Carry-over

In high-performance liquid chromatography (HPLC) tests, carry-over poses a significant challenge, stemming from residues that may adhere within the chromatographic separation system.<sup>53</sup> This issue can lead to contamination of subsequent samples, particularly those with lower concentrations or blank samples, potentially compromising the integrity of the analysis. Effective resolution or mitigation of this problem is paramount in such analyses. In the carry-over validation assay, the desorption peak areas for LAM and IS in blank samples analyzed before any setup were 1003 and 4920, respectively. For comparison, the LLOQ and IS areas of 35908 and 5270257, respectively, were also obtained. After the ULOQ (2872851) and IS (5387863) areas were obtained, the initial blank sample was reanalyzed twice, resulting in desorption peak areas of 570 and 1135 for LAM and 4677 and 3901 for IS, respectively. Notably, our results demonstrated robust

performance with no desorption peak areas exceeding the established thresholds of 20% of the lower limit of quantification (LLOQ) for LAM or 5% for IS. This outcome underscores the efficiency of the LDTD-MS/MS analysis system compared to HPLC<sup>17</sup> coupled with MS/MS systems. Unlike the latter, which necessitates extensive washing of the injection needle with various solvents, resulting in up to a minute increase in analysis time, the simplicity of the LDTD-MS/MS system contributes to reduced risk of carry-over contamination.

## Stability

Outcomes of the stability studies indicate that LAM concentrations remained consistent under the applied stress conditions, maintaining integrity at both concentration levels (HQC and LQC). Furthermore, when stored at room temperature (20 °C), LAM demonstrated stability in plasma samples for up to 4 h. Post-sample preparation at 20 °C, LAM retained stability for 1.96 h in post-preparative stability assessments. Moreover, LAM exhibited no significant fluctuations in LAM concentrations even after undergoing four complete freeze-thaw cycles, or during a 2.5-month long-term stability test, as well as the aforementioned stability tests, with analyte content consistently within 15% of the nominal concentration. Table 2 displays a comprehensive overview of all stability results.

Our consistent validation results substantiate the selection of LDTD-MS/MS over conventional HPLC-MS/MS, owing to its enhanced analytical speed, reduced solvent consumption, and greater suitability for the specific analyte under investigation. The validation results presented in this study confirm that this method meets the requirements outlined in RDC 27/2012, fully adhering to the regulatory

**Table 2.** Overview of LAM stability in human plasma under various laboratory conditions

Stability test	Sample	Measured concentration $\pm$ SD / (ng mL <sup>-1</sup> )	RE / %
Freeze-thaw cycles (4 cycles)	LQC	63.1 $\pm$ 3.76	5.19
	HQC	1716.7 $\pm$ 40.50	7.29
Short-term (06.58 h/20 °C)	LQC	59.6 $\pm$ 4.25	-0.67
	HQC	1625.0 $\pm$ 131.26	1.56
Post-preparative stability (LDTD plate for 1.93 h, and ca. 20 °C)	LQC	62.3 $\pm$ 2.71	3.83
	HQC	1684.7 $\pm$ 100.85	5.29
Long-term stability (2.5 months at -70 $\pm$ 15 °C)	LQC	54.83 $\pm$ 4.13	-8.61
	HQC	1460.82 $\pm$ 105.66	-8.70

Stability results of LAM in human plasma under various temperatures and storage conditions (n = 6, mean  $\pm$  SD) at concentrations of 60 ng mL<sup>-1</sup> (low-quality control) and 1600 ng mL<sup>-1</sup> (high-quality control). samples Relative error (RE%), calculated as the percentage difference between measured and nominal concentrations, was used to determine stability. SD: standard deviation; LDTD: laser diode thermal desorption; LQC: low concentration; HQC: high concentration.

standards established by ANVISA,<sup>38</sup> thereby demonstrating its scientific and regulatory robustness for the intended application.

While our LDTD-MS/MS approach proved highly versatile and adaptable, it is essential to address its current limitations, particularly to meet the ICH M10<sup>39</sup> guideline updates: Incurred Sample Reanalysis (ISR) and cross-validation. At the time this study was conducted, these requirements had not yet been incorporated into the regulatory framework of ANVISA.<sup>38</sup> ISR is particularly relevant for studies involving high sample heterogeneity, where variability in plasma protein binding, endogenous compounds, or matrix effects may compromise the consistency between validation and research samples. Similarly, cross-validation is critical when methodological changes, such as using LDTD-MS/MS instead of HPLC-MS/MS, significantly alter analytical conditions, warranting comparative evaluations across platforms.<sup>38,54</sup>

As ANVISA aligns with the updated ICH M10 guidelines, integrating these additional assessments into future studies will strengthen the reliability, flexibility, and compliance of the method with evolving global regulatory expectations and the dynamic landscape of bioanalytical science.

Clinical application of the LDTD-MS/MS method in a comparative PK study

The developed and validated LDTD-MS/MS method proved effective in a clinical trial, enabling the assessment of the PK of two distinct oral tablet formulations of LAM. Through this method, precise quantification of LAM concentrations within the linearity range of 20 to 2000 ng mL<sup>-1</sup> was achieved for a duration of up to 96 h post-administration of the formulations. Overall, compared

to previously reported methods for quantifying LAM in plasma samples as such,<sup>42,55,56</sup> our method offers several significant advantages. These include the use of a tiny biological sample volume, a straightforward extraction procedure with enhanced sensitivity, a large dynamic range, and the shortest total analysis time reported for this drug. To the best of our knowledge, this is the first bioanalytical method utilizing LDTD-MS/MS for the quantitation of this antiepileptic drug in human plasma.

Figure 4 illustrates the mean plasma concentration-time profiles of LAM following a single oral dose of the reference formulation and the test tablet formulation, respectively. The primary PK parameters of LAM for the tablet formulations are summarized in Table 3.

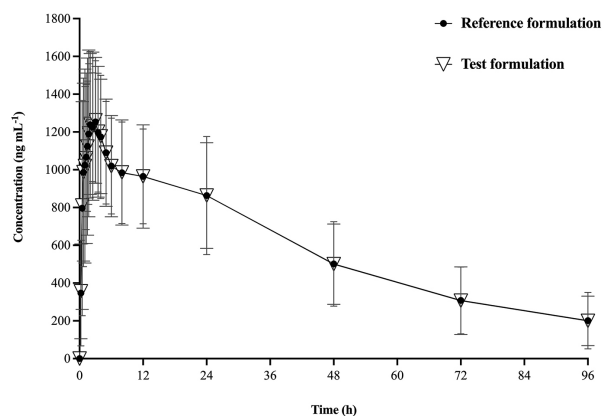


**Figure 4.** The pharmacokinetic profile of LAM following oral administration of two different formulations is depicted as plasma concentration *versus* time (area under curve from zero to 96 h, AUC<sub>0-96</sub>). The reference formulation (●) and the test formulation (▽) were each administered as a single 100 mg dose to 36 healthy, fasting volunteers. The two groups did not show any meaningful distinctions. Vertical bars indicate mean standard error.

The PK analysis demonstrated comparable performance between the reference and test tablet formulations of

**Table 3.** Key pharmacokinetics (PK) parameters of LAM following a 100 mg dose of reference and test tablet formulations in healthy volunteers

PK parameter	Method of calculating	Reference		Test	
		Average	SD	Average	SD
AUC <sub>0-96</sub> / (ng mL <sup>-1</sup> h)	trapezoids	55469.78	17497.8	51616.36	17202.21
T <sub>max</sub> / h	observed	1.66	0.62	2.45	0.72
C <sub>max</sub> / (ng mL <sup>-1</sup> )	observed	1516.42	361.34	1425.41	373.36
Vz/F / L	$\frac{Cl}{F} / ke$	80.77	22.97	83.77	14.93
Cl/F / (L h <sup>-1</sup> )	dose/AUC	1.77	0.57	1.96	0.69
t <sub>1/2</sub> / h	0.693/ke	35.09	8.40	33.71	6.73

Plasma PK characteristics of LAM under fasting conditions. AUC<sub>0-96</sub>: area under the plasma concentration-time curve after the last dose from zero time to the last time point of 96 h; T<sub>max</sub>: observed time to reach C<sub>max</sub>; C<sub>max</sub>: maximum observed plasma concentration after drug administration; Vz/F: apparent volume of distribution; CL/F: the apparent clearance; t<sub>1/2</sub>: drug half-life, ke: elimination rate constant, often obtained from the slope of the terminal phase of a semi-logarithmic plasma concentration-time curve, and 0.693 = natural logarithm of 2. PK parameters were calculated by the non-compartmental analysis. SD: standard deviation.

LAM. Both formulations achieved similar drug exposure, as reflected in their area under curve (AUC) values, with slightly different  $T_{\max}$  and  $C_{\max}$  (maximum observed plasma concentration after drug administration). The apparent clearance (CL/F) and volume of distribution (Vz/F) were also closely aligned, suggesting comparable drug distribution and elimination profiles. The findings indicate that the formulations presented similar absorption, distribution, and clearance.

The PK results also show that drug half-life ( $t_{1/2}$ ) of both the reference and test formulations exceeds 24 h, confirming the classification of LAM as a long half-life drug under established guidelines. Such data confirms the suitability of the method and the robustness of the experimental design, supporting the use of the truncated AUCs for long  $t_{1/2}$  drugs to ensure comparability of absorption processes while minimizing unnecessary and potentially unethical prolonged sampling periods.<sup>57-60</sup>

Moreover, the PK profile obtained aligns with previous studies on oral administration of LAM in healthy volunteers.<sup>40,61,62</sup>

## Conclusions

A rapid, high-throughput method for quantifying LAM in human plasma using LDTD-MS/MS was successfully developed and validated. LDTD-MS/MS offers key advantages, including minimal plasma volume requirements, high sensitivity, repeatability, low matrix interference, and adequate LAM and IS selectivity. Our method features a more sustainable approach by bypassing the chromatographic separation process. Effective sample cleanup was achieved through an optimized extraction method, simplifying the process and enhancing specificity with LDTD-MS/MS analysis. The linearity range of 20 to 2000 ng mL<sup>-1</sup> was suitable for quantifying LAM in human plasma for up to 96 h, enabling the determination of key PK parameters for two different oral formulations. In our current state of knowledge, this study represents the first literature report of a bioanalytical method for quantitating LAM using LDTD-MS/MS. Looking toward the future, we plan to develop and validate LDTD-MS/MS methods that integrate the latest ICH M10 guideline recommendations, including cross-validation and ISR. By addressing these essential aspects, we aim to strengthen the alignment of this approach with global standards and explore its potential applications in bioanalysis and beyond.

## Acknowledgments

The authors would like to thank Fundação de Amparo

à Pesquisa do Estado de Goiás (FAPEG), the Coordenação de Aperfeiçoamento de Pessoal de Nível Superior (CAPES), and especially acknowledge the Instituto de Ciências Farmacêuticas (ICF) for providing support in the form of analytical and clinical data used in this study. The bioanalytical method and pharmacokinetic data presented in this manuscript were generated as part of an exploratory study on the LDTD-MS/MS method, conducted independently of regulatory submissions or marketing approval processes for any drug or pharmaceutical product.

## Author Contributions

Glauco César F. F. Soares and Danillo F. M. C. Veloso contributed equally to conceptualization, formal analysis, investigation, data curation, writing (original draft, review, and editing), and visualization; Iram M. Mundim was involved in conceptualization, investigation, data curation, and writing (review and editing); Maria Carolina Almeida contributed to formal analysis, methodology, validation, visualization, and writing (review and editing); Leonardo S. Teixeira and Luiz Carlos da Cunha were responsible for conceptualization, investigation, writing (original draft, review, and editing), visualization, and supervision.

## References

1. Picard, P.; Letarte, S.; Rochon, J.; Paquin, R. E. In *High-Throughput Mass Spectrometry in Drug Discovery*, 1<sup>st</sup> ed.; Liu, C.; Zhang, H., eds.; John Wiley & Sons, Inc.: London, UK, 2023. [Link] accessed in February 2025
2. Joh, S.; Na, H.-K.; Son, J. G.; Lee, A. Y.; Ahn, C.-H.; Ji, D.-J.; Wi, J.-S.; Jeong, M. S.; Lee, S.-G.; Lee, T. G.; *ACS Nano* **2021**, *15*, 10141. [Crossref]
3. Wang, H.; Zhao, X.; Huang, Y.; Liao, J.; Liu, Y.; Pan, Y.; *Analyst* **2020**, *145*, 2168. [Crossref]
4. Andersen, W. C.; VanSickle, M.; Storey, J.; Sheldon, V.; Lohne, J.; Turnipseed, S. B.; Thomas, T.; Madson, M.; *Food Addit. Contam., Part A* **2019**, *36*, 1616. [Crossref]
5. Bořík, A.; Nováková, P.; Stroski, K. M.; *Rapid Commun. Mass Spectrom.* **2023**, e9517. [Crossref]
6. da Silva, C. T. A.; Lustosa A. I.; Kogawa, C. A.; *Curr. Pharm. Des.* **2023**, *29*, 1166. [Crossref]
7. Vervoort, N.; Goossens, K.; Baeten, M.; Chen, Q.; *Anal. Sci. Adv.* **2021**, *2*, 109. [Crossref]
8. Cantor, S. L.; Gupta, A.; Khan, M. A.; *J. Pharm. Sci.* **2014**, *103*, 539. [Crossref]
9. Kaya, S. I.; Cetinkaya, A.; Ozkan, S. A.; *Trends Environ. Anal. Chem.* **2022**, *33*, e00157. [Crossref]
10. Sinzervinch, A.; Torres, M. S. I.; Kogawa, C. A.; *Curr. Pharm. Des.* **2023**, *29*, 2442. [Crossref]

11. Branstetter, L.; Chatterjee, C.; Higgins, M. J.; *Res. Policy* **2022**, *51*, 104595. [Crossref]
12. Zhou, S.; Li, R.; Chen, Z.; Ren, R.; Wang, X.; Dai, Q.; Wen, D.; Guan, Y.; Zhang, X.; Tang, S.; Zhou, L.; Huang, M.; *Biomed. Chromatogr.* **2022**, *36*, e5393. [Crossref]
13. Milosheška, D.; Roškar, R.; Vovk, T.; Lorber, B.; Grabnar, I.; Trontelj, J.; *Pharmaceuticals* **2024**, *17*, 449. [Crossref]
14. Shi, X.; Zhang, D.; Zhao, Z.; Mei, S.; *Bioanalysis* **2024**, *16*, 233. [Crossref]
15. Wong, J. M.; Jones, J. W.; Jiang, W.; Polli, J. E.; Kane, M. A.; *Ther. Drug Monit.* **2015**, *37*. [Crossref]
16. Hirano, L. Q. L.; de Oliveira, A. L. R.; de Barros, R. F.; Veloso, D. F. M. C.; Lima, E. M.; Santos, A. L. Q.; Moreno, J. C. D.; *J. Vet. Pharmacol. Ther.* **2024**, *47*, 427. [Crossref]
17. Heudi, O.; Barteau, S.; Picard, P.; Tremblay, P.; Picard, F.; Kretz, O.; *J. Pharm. Biomed. Anal.* **2011**, *54*, 1088. [Crossref]
18. Dion-Fortier, A.; Gravel, A.; Guérette, C.; Chevillot, F.; Blais, S.; Auger, S.; Picard, P.; Segura, P. A.; *J. Mass Spectrom.* **2019**, *54*, 167. [Crossref]
19. Choi, H.; Lee, D.; Kim, Y.; Nguyen, H.-Q.; Han, S.; Kim, J.; *J. Am. Soc. Mass Spectrom.* **2019**, *30*, 1174. [Crossref]
20. Springer, V.; Zhou, Y.; Aguilera, Á. Y.; Emmer, Å.; *Anal. Bioanal. Chem.* **2024**, *416*, 861. [Crossref]
21. Luo, X.; Tue, P.-T.; Sugiyama, K.; Takamura, Y.; *Sci. Rep.* **2017**, *7*, 15170. [Crossref]
22. Badjagbo, K.; Sauvé, S.; *Anal. Chem.* **2012**, *84*, 5731. [Crossref]
23. Boisvert, M.; Fayad, P. B.; Sauvé, S.; *Anal. Chim. Acta* **2012**, *754*, 75. [Crossref]
24. Yao, J.; Scott, J. R.; Young, M. K.; Wilkins, C. L.; *J. Am. Soc. Mass Spectrom.* **1998**, *9*, 805. [Crossref]
25. Peterson, D. S.; *Mass Spectrom. Rev.* **2007**, *26*, 19. [Crossref]
26. Sahasrabudde, A.; Oakley, D.; Chen, K.; McCarter, J. D.; *SLAS Discovery* **2021**, *26*, 230. [Crossref]
27. Lonappan, L.; Pulicharla, R.; Rouissi, T.; Brar, S. K.; Verma, M.; Surampalli, R. Y.; Valero, J. R.; *J. Chromatogr. A* **2016**, *1433*, 106. [Crossref]
28. Feist, P.; Hummon, A. B.; *Int. J. Mol. Sci.* **2015**, *16*, 3537. [Crossref]
29. Bynum, N. D.; Moore, K. N.; Grabenauer, M.; *J. Anal. Toxicol.* **2014**, *38*, 528. [Crossref]
30. Segura, P. A.; Guillaumain, C.; Eysseric, E.; Boudrias, J.; Moreau, M.; Guérette, C.; Clémencin, R.; Beaudry, F.; *Rapid Commun. Mass Spectrom.* **2022**, *36*, e9373. [Crossref]
31. Cohen, A. F.; Land, G. S.; Breimer, D. D.; Yuen, W. C.; Winton, C.; Peck, A. W.; *Clin. Pharmacol. Ther.* **1987**, *42*, 535. [Crossref]
32. Michail, K.; Daabees, H. M.; Beltagy, Y.; Abdel-Khalek, M.; Khamis, M. M.; *J. Chem.* **2013**, *2013*, 608196. [Crossref]
33. Peck, A. W.; *Epilepsia* **1991**, *32*, S9. [Crossref]
34. Costa, B.; Silva, I.; Oliveira, J. C.; Reguengo, H.; Vale, N.; *Sci. Pharm.* **2024**, *92*, 15. [Crossref]
35. *Analyst*, version 1.7.2; AB SCIEX, Framingham, MA, 2020.
36. U.S. Department of Health and Human Services Food and Drug Administration (US FDA); Center for Drug Evaluation and Research (CDER); *Bioanalytical Method Validation Guidance for Industry*, <https://www.fda.gov/files/drugs/published/Bioanalytical-Method-Validation-Guidance-for-Industry.pdf>, accessed in February 2025.
37. Visconti, G.; Boccard, J.; Feinberg, M.; Rudaz, S.; *Anal. Chim. Acta* **2023**, *1240*, 340711. [Crossref]
38. Agência Nacional de Vigilância Sanitária (ANVISA); Resolução da Diretoria Colegiada (RDC) No. 27, de 17 de maio de 2012, *Dispõe Sobre os Requisitos Mínimos para a Validação de Métodos Bioanalíticos Empregados em Estudos Com Fins de Registro e Pós-Registro de Medicamentos*; Diário Oficial da União (DOU), Brasília, 2012. [Link] accessed in February 2025
39. International Council for Harmonisation of Technical Requirements for Pharmaceuticals for Human Use (ICH); *ICH Guideline M10 on Bioanalytical Method Validation and Study Sample Analysis*; [https://database.ich.org/sites/default/files/M10\\_Guideline\\_Step4\\_2022\\_0524.pdf](https://database.ich.org/sites/default/files/M10_Guideline_Step4_2022_0524.pdf), accessed in February 2025.
40. Methaneethorn, J.; Leelakanok, N.; *Seizure* **2020**, *82*, 133. [Crossref]
41. Hotha, K. K.; Kumar, S. S.; Bharathi, D. V.; Venkateswarulu, V.; *Biomed. Chromatogr.* **2012**, *26*, 491. [Crossref]
42. Fang, L.; Li, Z.; Kinjo, M.; Lomonaco, S.; Zheng, N.; Jiang, W.; Zhao, L.; *Epilepsia* **2023**, *64*, 152. [Crossref]
43. Benedetti, N. I. G. M.; Veloso, D. F. M. C.; Nascimento, L. T.; Almeida Diniz, G. D.; Maione-Silva, L.; Lima, M. E.; *Curr. Pharm. Anal.* **2020**, *16*, 623. [Crossref]
44. *Phoenix WinNonlin*, version 6.4.0.768; Pharsight, Mountain View, CA, 2008.
45. Ghatol, S.; Vithlani, V.; Gurule, S.; Khuroo, A.; Monif, T.; Partani, P.; *J. Pharm. Anal.* **2013**, *3*, 75. [Crossref]
46. Kempka, M.; Sjö Dahl, J.; Björk, A.; Roeraade, J.; *Rapid Commun. Mass Spectrom.* **2004**, *18*, 1208. [Crossref]
47. Williams-Pavlatos, K.; Wesdemiotis, C.; *Adv. Sample Prep.* **2023**, *7*, 100088. [Crossref]
48. Tholey, A.; Heinzle, E.; *Anal. Bioanal. Chem.* **2006**, *386*, 24. [Crossref]
49. Timofeeva, I.; Shishov, A.; Kanashina, D.; Dzema, D.; Bulatov, A.; *Talanta* **2017**, *167*, 761. [Crossref]
50. Lin, H.; Lin, L.; Xu, L.; Xie, Y.; Xia, Z.; Wu, Q.; *J. Tradit. Chin. Med. Sci.* **2018**, *5*, 291. [Crossref]
51. Liu, W.; Nie, H.; Liang, D.; Bai, Y.; Liu, H.; *Talanta* **2020**, *209*, 120357. [Crossref]
52. Li, M.; Wang, H.; Huan, X.; Cao, N.; Guan, H.; Zhang, H.; Cheng, X.; Wang, C.; *Anal. Bioanal. Chem.* **2021**, *413*, 5871. [Crossref]

53. Jogpethe, A.; Jadav, T.; Rajput, N.; Kumar Sahu, A.; Tekade, R. K.; Sengupta, P.; *Microchem. J.* **2022**, *179*, 107464. [Crossref]
54. Fjording, M. S.; Goodman, J.; Briscoe, C.; *Bioanalysis* **2024**, *17*, 1. [Crossref]
55. Ventura, S.; Rodrigues, M.; Pousinho, S.; Falcão, A.; Alves, G.; *Microchem. J.* **2017**, *130*, 221. [Crossref]
56. Castel-Branco, M. M.; Almeida, A. M.; Falcão, A. C.; Macedo, T. A.; Caramona, M. M.; Lopez, F. G.; *J. Chromatogr. B: Biomed. Sci. Appl.* **2001**, *755*, 119. [Crossref]
57. Rossen Koytchev, U. E.; *Arzneimittelforschung Drug Res.* **2011**, *58*, 255. [Crossref]
58. Daher, A.; Pinto, D. P.; da Fonseca, L. B.; Pereira, H. M.; da Silva, D. M. D.; da Silva, L. S. F. V.; Esteves, A. L.; Soares Medeiros, J. J.; Mendonça, J. S.; *Malaria J.* **2022**, *21*, 16. [Crossref]
59. Ju, G.; Yan, K.; Xu, Y.; Chen, S.; Zheng, Z.; Qiu, W.; *Drug Des. Devel. Ther.* **2020**, *14*, 2637. [Crossref]
60. U.S. Department of Health and Human Services Food and Drug Administration (US FDA); Center for Drug Evaluation and Research (CDER); *Bioequivalence Studies with Pharmacokinetic Endpoints for Drugs Submitted Under an ANDA Guidance for Industry*, <https://www.fda.gov/media/87219/download> accessed in February 2025.
61. Garnett, W. R.; *J. Child Neurol.* **1997**, *12*, S10. [Crossref]
62. Ramsay, R. E.; Pellock, J. M.; Garnett, W. R.; Sanchez, R. M.; Valakas, A. M.; Wargin, W. A.; Lai, A. A.; Hubbell, J.; Chern, W. H.; Allsup, T.; Otto, V.; *Epilepsy Res.* **1991**, *10*, 191. [Crossref]

Submitted: January 31, 2025

Published online: March 11, 2025